A1 Astrocyte-Derived TNFα Drives OPC-like Differentiation of Neural Stem Cells after Ischemic Injury

Ashley Hein[1]

Received May 17, 2026
Accepted August 1, 2026
Electronic access August 15, 2026

The glial scar that forms after ischemic injury creates a structurally and functionally complex barrier, yet how it regulates neural stem cell (NSC) fate remains unclear. I combined single-cell RNA sequencing reanalysis of a mouse model with middle cerebral artery occlusion (MCAO) with in vitro experiments using iPSC-derived NSCs to examine astrocyte-NSC interactions. Computational analysis revealed a reduction in NSC populations alongside increased oligodendrocyte progenitor cells post-injury. I hypothesized that reactive astrocytes in the glial scar, specifically pro-inflammatory astrocyte states, promote NSC fate shifting towards an OPC-like phenotype. Reactive astrocytes are key scar components, traditionally classified as A1 (neurotoxic) or A2 (neuroprotective). Cell-cell communication analysis identified TNFα, a pro-inflammatory cytokine secreted around the scar, to be a significant signaling molecule between NSCs and A1 astrocytes upregulated after injury. In vitro, NSCs co-cultured with A1 astrocytes or exposed to A1-conditioned media (CM) increased expression of NG2+ oligodendrocyte precursor cell (OPC) markers, a cellular population that localizes to the scar periphery. TNFα alone similarly promoted this phenotype. A1 astrocytes were generated by stimulating homeostatic astrocytes with microglia-derived cytokines, leading to TNFα upregulation by reverse transcription quantitative polymerase chain reaction (RT-qPCR) and sustained secretion by enzyme-linked immunosorbent assay (ELISA). Only strongly stimulated astrocytes maintained elevated TNFα after one week, indicating a threshold-dependent feedback mechanism. In contrast, astrocytes stimulated under A2 conditions (TNFα + IL-1β) did not sustain TNFα secretion. Finally, pharmacological inhibition of astrocyte activation with dantrolene or salubrinal appeared to reduce TNFα release and expression, and abrogate its effect on NSCs. Together, these results support a model in which A1 reactive astrocytes influence NSC state and promote OPC-associated marker expression, with TNFα as a potential mediator. Additional lineage-tracing and loss-of-function experiments will be required to determine whether TNFα is necessary and sufficient for NSC fate conversion, and whether converted cells remain differentiated, localize to the site of the glial scar, and contribute to its function.

Introduction

In response to acute and chronic inflammation or insult to the central nervous system (CNS), a glial scar forms, a physical and biochemical barrier formed by reactive glial cells[1]. The main cell types surrounding the glial scar lesion are reactive astrocytes, reactive microglia, and a dense ring of OPCs[2]. They isolate infiltrating immune cells and remodel the extracellular matrix (ECM) to limit further injury[3]. However, the glial scar creates a neurotoxic environment over time. Able to persist for several months, the scar forms a physical and biochemical block to axon regeneration[4]. Detection of PAMPs (such as viral RNA or LPS) or DAMPs (such as ATP, misfolded proteins, or myelin debris) triggers microglia taking on a reactive phenotype characterized by a distinct inflammatory gene signature[5,6] Pro-inflammatory M1 reactive microglia secrete cytokines such as TNFα, IL-1α, IL-1β, and C1q[7], which trigger astrocytes to take on what has been traditionally simplified into two different reactive phenotypes[8]. While the A2 phenotype is neuroprotective, secreting neurotrophic factors like BDNF[9], A1 astrocytes have been previously thought to have minimal if any beneficial functions. Alongside an impaired ability to carry out regulatory functions of homeostatic astrocytes such as lactate and glutamate regulation, A1 astrocytes are thought to secrete an unidentified compound[10] that leads to neuronal cell death. Although the A1/A2 dichotomy overly simplifies a much larger continuum of reactive astrocytes states[11,12], it remains a useful experimental framework for capturing broad patterns in major astrocyte responses to CNS injury and disease.

NSCs are self-renewing, multipotent cells with the potential to differentiate into astrocytes, oligodendrocytes and neurons[13,14]. As a result of their sensitivity to inductive signaling, they tend to occupy specialized niches in the brain with regulated microenvironments that allow them to preserve multipotency, such as the subventricular zone (SVZ) lining the lateral ventricles and the subgranular zone (SGZ) of the dentate gyrus of the hippocampus[15]. NSC differentiation during glial scar

[1] *Weissman Lab, Stanford*

formation has previously been a relatively unexplored area of research. While it is accepted that inflammation generally results in NSCs forming a higher proportion of glial cells rather than neurons [16], the primarily signaling pathways resulting in this preference is an ongoing angle for investigation.

This project sought to address possible signaling molecules and cell types critical to directing NSC fate. Single-cell reanalysis of a murine model with a middle cerebral artery occlusion (MCAO) induced glial scar revealed a significant reduction in the number of NSCs in the aftermath of glial scar formation. This trend was consistent across multiple datasets, raising the question if NSCs were dying or being induced to differentiate, and what was the source of the inductive signal if they were specializing. Enrichment of other cell populations, particularly OPCs, supported the possibility of differentiation rather than cell death.

Upon examining key signaling pathways with NSCs as receivers, the TNFα signaling pathway between A1 reactive astrocytes and NSCs stood out to be significantly upregulated. This project examines the crucial interaction between A1 astrocytes and NSCs as the scar forms, contesting the notion that A1 astrocytes are purely detrimental and should be inhibited from formation [17,18].

Dantrolene and salubrinal were used to dampen TNFα release in reactive astrocytes. These are inhibitors that converge on the endoplasmic reticulum (ER) stress signaling pathway. Dantrolene's primary mechanism of action is stabilizing Ca2+ by blocking ryanodine receptors [19,20], reducing pro-inflammatory PERK activation, while salubrinal inhibits eIF2α dephosphorylation when PERK is active to give the ER time to clear and refold proteins [21].

Materials and Methods

Experiments were performed to test how factors secreted by M1 microglia and A1 astrocytes influence NSC differentiation. To further probe the interaction specifically between A1 astrocytes and NSCs, NSCs were given TNFα in isolation, incubated with CM from reactive astrocytes, and co-cultured in direct contact with reactive astrocytes. Cell lineage was cross-validated through both immunofluorescence microscopy (IF) and RT-qPCR.

Single-cell RNA-seq reanalysis

Publicly available single-cell RNA-seq data from a mouse MCAO model (3 sham, 3 MCAO; GSE174574) were processed in Seurat. Cells with $<$200 or $>$6,000 detected genes, as well as cells with $>$5% mitochondrial gene expression, were excluded. Data were log-normalized (NormalizeData), highly variable genes identified (FindVariableFeatures), and scaled (ScaleData). Elbow plots were generated to select the number of principal components to be 17 for principal component analysis (PCA). Graph-based clustering was performed using FindNeighbors (k = 15, dimensions 1-17) followed by FindClusters (resolution = 0.6). Clusters were annotated using established markers (log fold-change $\geq$ 0.5; $\geq$ 30% expressing cells). Cell-type proportions between conditions were compared using Welch's t-tests. For cell-cell communication, a CellChat object was created from normalized data and annotated cell types. Ligand-receptor interactions were inferred using the mouse database and filtered to retain pairs with $\geq$ 10% expression in sender or receiver populations, then aggregated into signaling pathways for communication probability analysis.

Table 1 Marker genes used to annotate cell types in scRNA-seq analysis.

Marker genes	Cell type
Aqp4, Gfap, Aldh1l1	Astrocytes
Mbp, Plp1, Mog	Oligodendrocytes
Pdgfra, Sox10, NG2	OPCs
Snap25, Syt1, Rbfox3	Neurons
Cx3cr1, Tmem119, P2ry12	Microglia
Pecam1, Cldn5	Endothelial cells
Foxj1, Dnah9	Ependymal cells
Pdgfrb, Rgs5	Pericytes
C3, Serpina3n, Vim, Lcn2, S100B	A1 Astrocytes
Emp1, Clcf1, Tgm1, Ptx3, S100a10	A2 Astrocytes
Nes, Sox2, Prom1	NSCs

Experiment #1: NSCs + A1/A2 factors

NSCs (ScTi003-A, STEMCELL Technologies) were grown in NSC maintenance media as floating neurospheres and passaged at $>$250 μm using Accutase. NSC identity was validated after two weeks through immunostaining on untreated cells, where $>$85% were found to be positive for a combination of NSC markers SOX2, Nestin, PAX6, and PROM1 while lacking robust expression of markers associated with neuronal or glial differentiation, such as βIII-tubulin, ALDH1L1, O4, MAP2, NEUN, OLIG2 and SOX10.

To test the combinations of cytokines released during glial scar formation on NSCs, NSCs were plated on Matrigel at a seeding density of 10k cells per well in 4 rows on a 96-well plate. After 24 h, cells were treated with A1 factors (TNFα,·IL-1α,·C1q) or A2 factors (IL-1β,·TNFα). Two control rows were maintained in either NSC medium or blank differentiation medium. After 48·h, factors were removed and cells were washed 8x with PBS, then differentiated for 2 weeks.

To IF, cells were fixed in 4% PFA (15 min), incubated in blocking buffer (1 h 45 min), incubated with primary antibodies overnight at 4°C, then secondary antibodies at room

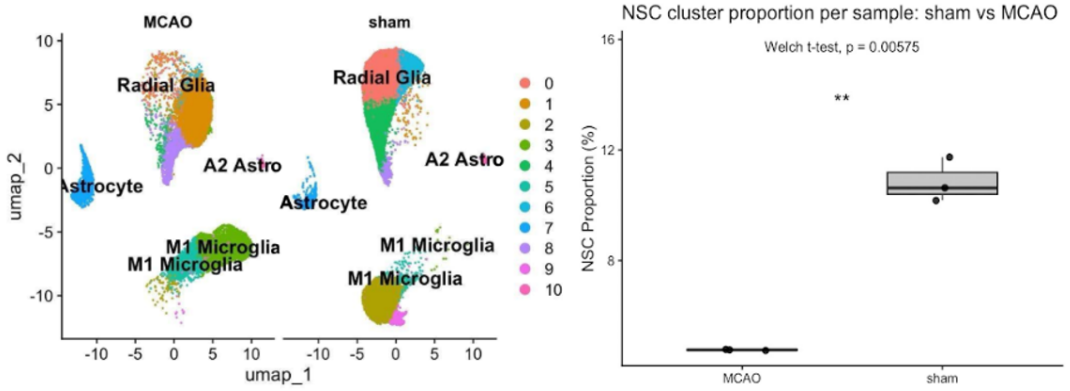

Figure. 1 Effect of glial scar on proportions of cells in the brain. As shown in the resulting uMAP, radial glia (NSC) populations were reduced in the group that underwent MCAO and subsequent glial scar formation. Qualitative analysis in R demonstrated this to be a significant difference (Welch's t-test, $p < 0.01$**). Data re-analyzed from Zhang et al., 2022, GSE174574.

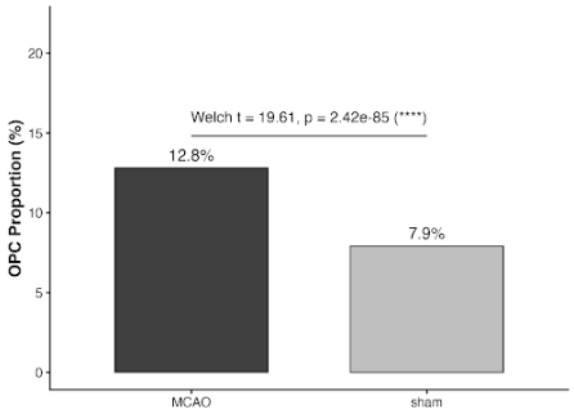

Figure. 2 The number of OPCs was found to be enriched in mice that had undergone MCAO (Welch's t-test, $p < 0.0001$****). This suggests the possibility that the NSCs may be differentiating into OPCs. Data re-analyzed from Zhang et al., 2022, GSE174574.

temperature (3 h). 4',6-diamidino-2-phenylindole (DAPI) was added to stain the nuclei in a 1:1000 dilution with staining buffer. Wells were washed 2 times and imaged on a LeicaLasX microscope.

Experiment #2: NSCs + individual factors

A1 factors were tested individually. NSCs were plated in five rows on a 96-well plate. One row received TNFα, one row IL-1α, and one row C1q. After 48 h of incubation with the cytokines, wells were washed 8x with PBS and media was replaced with normal NSC media. After 2 weeks, NSCs were fixed and stained.

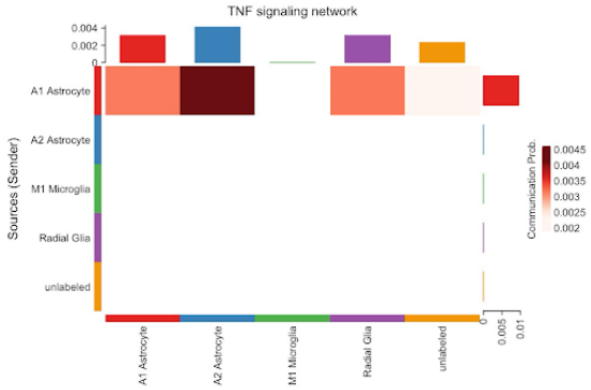

Figure. 3 Conflicting accounts in the literature report whether or not astrocytes are capable of TNFα secretion, with some sources arguing that astrocytes in mixed glial cultures produce little to no TNFα under conditions of LPS, IFN-γ, or IL-1β stimulation[22]. However, single-cell analysis using CellChat demonstrated A1 reactive astrocytes to not only secrete TNFα but constitute the primary TNFα-secreting population at the 24-hour mark post injury. Experimental data also confirmed A1 reactive astrocytes are able to express and secrete TNFα. Data re-analyzed from Zhang et al., 2022, GSE174574.

Experiment #3: TNFα release by reactive astrocytes

Homeostatic, A1, and A2 reactive astrocytes were generated. Astrocytes were administered activating cytokines on a range of concentrations, using a serial dilution to test cytokine concentrations of 0.25x, 0.5x, 1x, 2x, 4x, 8x, and 16x. The 1x concentration was 30 ng/mL for TNFα, 3 ng/mL for IL-1α, 30 ng/mL for IL-1β, and 400 ng/mL for C1q, mimicking the protocol used by Liddelow et al. (2017) for generating reac-

tive astrocytes in vitro.

Activation with individual factors was also tested. Titration experiments comparing 4, 6, 8, and 10 PBS washes showed that in acellular Matrigel plates that received the same range of TNFα concentrations, 8 washes eliminated any traces of recombinant TNFα to below the threshold detectable by the ELISA kit, supporting that the TNFα later measured was endogenous rather than residual. Furthermore, a trypan blue live-dead count showed that astrocyte cultures subjected to 8 PBS washes maintained >90% viability. Dantrolene and salubrinal were dissolved in DMSO and applied at 3μM or 10μM to A1 astrocytes for 24 h after factor removal; vehicle controls received an equivolume DMSO. Wells were then washed 8x with PBS, returned to fresh astrocyte media, and CM was collected after 24 h and again after 7 days.

CM from all treatment groups was analyzed using a Human TNF alpha ELISA Kit (Invitrogen, KHC3013).

Experiment #4: NSCs + astrocyte CM

NSCs were plated on Matrigel in a 24-well plate and differentiated into astrocytes for 2 weeks with BMP4 and CNTF. Astrocytes were then activated with A1 or A2 factors, with homeostatic astrocytes as controls. After 5 days, factors were removed and some A1 astrocytes received 3μM or 10μM of dantrolene or salubrinal for 24 h, followed by 8x PBS washes and replacement with NSC media. After 24 h, CM was collected and 180 μL per well was applied to NSCs plated in Matrigel in a 96-well plate. NSCs were left to differentiate for 6 days, then fixed and stained or collected for RT-qPCR. rNA was extracted using the QIAGEN RNeasy kit, quantified by NanoDrop (typically 100 ng/μL, with acceptable 260/280 ratios) and reverse-transcribed with the High-Capacity RNA-to-cDNA kit (Thermo Fisher). RT-qPCR was then performed using PowerTrack 2x SYBR Green Master Mix. 3.5 μL of cDNA, 2 μL of indicator dye, and 29.5 μL of ultra-pure water were added to a total volume of 35 μL. Primers were prepared by adding 8 μL forward primer, 8 μL reverse primer, and 84 μL of ultra-pure water. 17.5 μL of the diluted primers were added to 175 μL SYBR Green and 122.5 μL of ultra-pure water before combined with cDNA to a 384-well plate. The ThermoCycler protocol was 37°C for 60 minutes, 95°C for 5 minutes, and 4°C for 30 minutes.

Experiment #5: NSCs + astrocyte co-culture

NSCs were transfected with a GFP$^+$ lentivirus and co-cultured with homeostatic, A1, or A2 reactive astrocytes. Astrocytes were activated for 5 days, washed 8x with PBS, and then seeded with NSCs at a 1:1 ratio (10,000 cells each) in 96-well plates in NSC media. After 6 days, co-cultures were separated for downstream analysis using Flow Cytometry, gating for GFP$^+$ NSCs versus GFP- astrocytes.

NSC process complexity was quantified in ImageJ. A binary mask of all cell processes was created and skeletonized. Then, the GFP-nuclear channel was examined to delete ROIs that lacked a GFP$^+$ nucleus. Running AnalyzeSkeleton on the remaining skeletons yielded a Results table reporting the number of branches and average branch length per skeleton.

Image Quantification and Statistical Analysis

All experiments were performed with three independent biological replicates. For IF, ten fields of view were acquired per well and averaged to yield the image-based quantifications presented for each biological replicate. Cells were identified based on DAPI staining, and binary masks (minimum object size of 20 μm^2, circularity 0.3-1.0) were used to quantify the percentage of positive cells and mean fluorescence intensity per cell. Images were set to the same minimum and maximum intensity before comparison.

Error bars represent standard deviation. Two-tailed Welch's t-tests were used for comparisons between two groups, while comparisons between more than two groups used one-way ANOVA with Tukey's post-hoc test. P-values of <0.05 were determined to be significant.

Table 2 Materials for cell culture and IF; key software and analytical tools used for scRNA-seq reanalysis, imaging, and quantification.

Astrocyte media	*NSC media*
PVA 90% 480 μL	DMEM/F12 500 ml
NAC 100x 480 μL	Neurobasal 500 μL
Neurobasal (L glutamine) 24 mL	N2 5 mL
DMEM / F12 (1:1) 24 mL	B27 (50x) 20 mL
N2 Supplement 480 μL	Glutamax 10 mL
B27 (Vit-A) 960 μL	Penn Strep 10 mL
hEGF 48 μL	hEGF(20 ug/mL) 1 mL
ITSX Insulin 480 μL	FGF2(20 ug/mL) 1 mL
Blocking Buffer	*Staining Buffer*
5 mL 3% Triton X-100	16.6 mL blocking buffer
1.5 mL horse serum	33.4 mL 1x TBS
43.5 mL 1x TBS	
Blank differentiation media	*Computational tools*
DMEM/F12 500mL	R Studio for single-cell sequencing, using datasets downloaded from NCBI
Neurobasal Medium 500mL	
GlutaMAX 10mL	ImageJ for editing immunofluorescence microscopy images and AnalyzeSkeleton to compare relative branch length between A1 and A2 astrocytes.
MEM-NEAA (100x) 10mL	
2-mercaptoethanol 0.5mL	
N2 5mL	
B27 -VitA (50x) 20mL	
2-p-L-AA (100x) 10mL	

Results

Experiment #1: NSCs + A1/A2 factors

After two weeks of differentiation, A1-treated NSCs exhibited a significantly higher proportion of C3[3] cells (68.3% $\pm$ 6.1%)

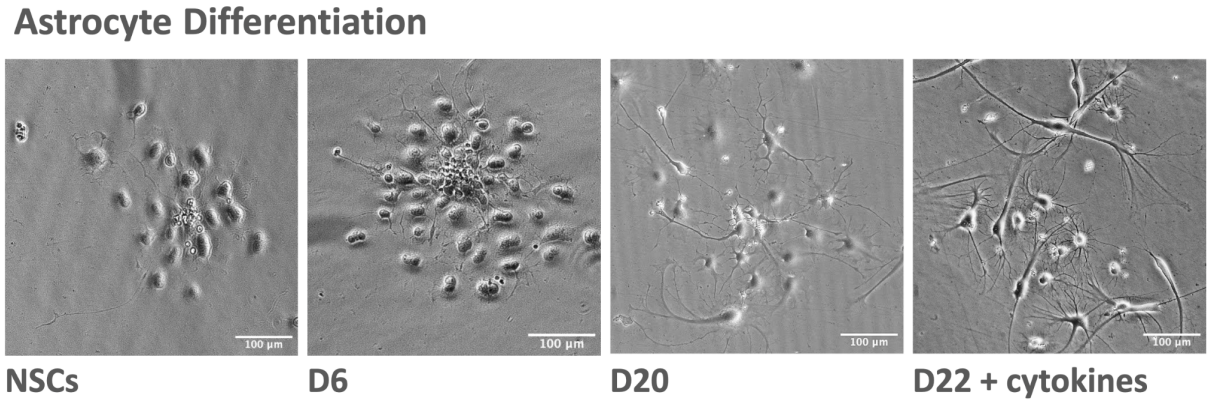

Figure. 4 Brightfield images of astrocyte differentiation and activation from iPSC-derived NSCs.

Table 3 Primary antibodies used for IF to identify NSCs, OPCs, and reactive astrocyte markers (A1-like and A2-like states).

Target	Cell Type	Supplier	Product Code	Concentration
OLIG2	OPC	Abcam	ab109186	1:500
SOX10	OPC	Abcam	ab227680	1:300
C3	A1 Astrocyte	Invitrogen	PA5-114921	1:300
S100A10	A2 Astrocyte	Invitrogen	MA5-15326	1:500
S100B	A1 Astrocyte	Abcam	ab52642	1:500
Nestin	A1 Astrocyte, NSC	Abcam	ab22035	1:500
SOX2	NSC	Abcam	ab97959	1:500
GFAP	NSC	Abcam	ab4674	1:5000
PDGFRA	OPC	Abcam	ab203491	1:500

than control (5.4% $\pm$ 1.8%) or A2-treated cells (7.1% $\pm$ 2.3%) (one-way ANOVA with Tukey's post hoc test, $p < 0.001$***). Most $C3^3$ cells (72.5% $\pm$ 5.8%) were also PDGFRA$^+$ of $C3^3$ cells were also PDGFRA$^+$, and exhibited increased branching phenotypically characteristic of the dense, fibrous web around the site of the glial scar.

Experiment #2: NSCs + individual factors

TNFα-treated NSCs upregulated OPC-associated markers relative to IL-1α or C1q. TNFα-treated NSCs exhibited both higher PDGFRA mean fluorescence intensity (0.758 $\pm$ 0.036 vs. 590 $\pm$ 0.032 for C1q and 0.187 $\pm$ 0.014 for IL-1α) and a greater fraction of PDGFRA$^+$ cells (0.761 $\pm$ 0.017 vs 0.363 $\pm$ 0.016 and 0.026 $\pm$ 0.002 respectively; one-way ANOVA with Tukey post hoc, all $p < 0.01$**). In contrast, IL-1α-treated NSCs showed low PDGFRA and SOX10 but robust expression of A1-associated markers GFAP and C3, with SOX2 expression restricted to this group.

Experiment #3: TNFα release by reactive astrocytes

Astrocytes stimulated with the highest cytokine concentrations exhibited the most sustained release of TNFα after 7 days. Out of the astrocytes that had received TNFα, IL-1α, or C1q alone only the group that had received TNFα demonstrated significant TNFα release after 24 h as well as after a week. However, A2 astrocytes given TNFα and IL-1β in combination did not release TNFα. Dantrolene and salubrinal reduced TNFα release by ELISA and TNFα mRNA and other A1-associated inflammatory markers by RT-qPCR.

Experiment #4: NSCs + astrocyte CM

A1 astrocyte CM increased PDGFRA$^+$ NSCs (58.9% $\pm$ 6.0%) compared to homeostatic CM (9.6% $\pm$ 3.8%) and A2 CM (22.3% $\pm$ 4.1%) ($p < 0.001$***). SOX10$^+$ cells similarly increased (54.1% $\pm$ 5.7% vs 7.2% $\pm$ 3.5% and 20.5% $\pm$ 3.9%, respectively). Mean fluorescence intensity for both markers increased by approximately 2-fold. CM from inhibitor-treated A1 astrocytes abrogated these effects, preserved multipotent markers, and allowed neurosphere-like aggregate formation.

Experiment #5: NSC + reactive astrocyte co-cultures

NSCs co-cultured with A1 astrocytes demonstrated increased proliferation, as shown by a higher percentage of GFP$^+$ cells despite all groups being seeded 1:1. Additionally, this group exhibited longer average branch lengths (6.48 $\pm$ 5.98 μm; n = 10,851 branches) than those with A2 astrocytes (1.66 $\pm$ 1.64 μm; n = 8,882 branches). A1 co=cultures also showed higher PDGFRA and lower NEUROD1 expression relative to homeostatic co-cultures.

Discussion and future directions

This study identifies a key signaling pathway between A1 reactive astrocytes and NSCs that is upregulated during glial scar formation. Through direct exposure to as well as experiments involving conditioned media and co-cultures, TNFα from A1 astrocytes drove NSCs to increase expression of

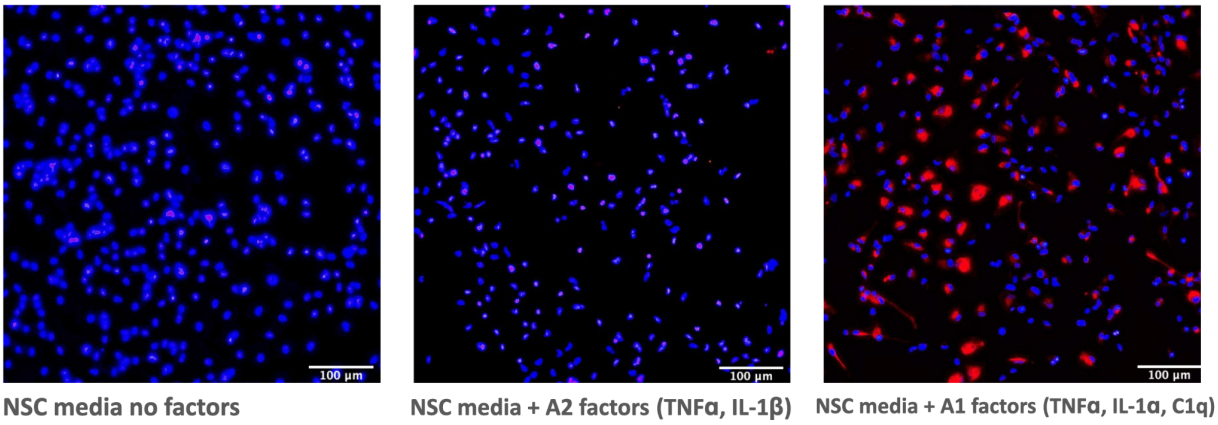

Figure. 5 NSCs given A1 factors express C3. NSCs that had been given NSC media + A1 factors were C3[3], while NSCs that had been given NSC media, blank differentiation media, or NSC media + A2 factors expressed no C3. C3 is shown in red; blue is DAPI used to stain cell nuclei.

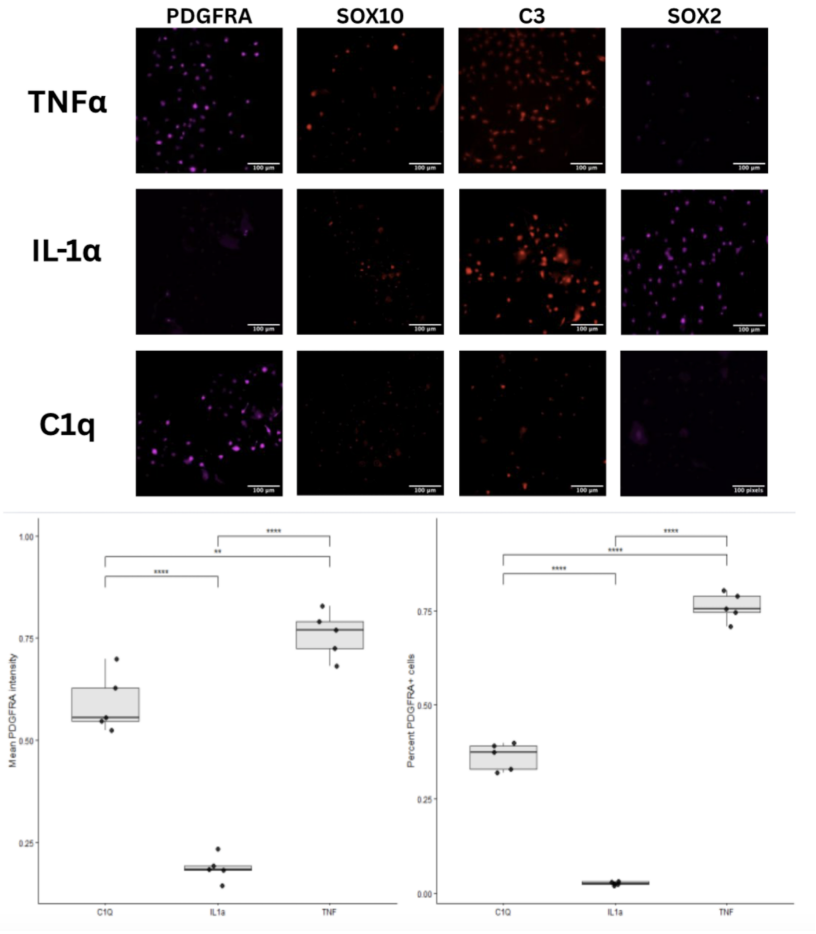

Figure. 6 (A) Effect of individual factors given directly to NSCs. TNFα resulted in upregulation of PDGFRA and SOX10, suggestive of OPCs. (B) Image analysis in ImageJ and R demonstrated the percent of cells expressing as well as the average mean intensity to be increased among TNFα-treated NSCs. IL-1α resulted in upregulation of C3, SOX2, and GFAP suggestive of A1 astrocytes.

Table 4 Cytokines, inhibitors, reagents, cells, and kits used.

Reagent	Use	Supplier	Catalogue Number
TNFα	A1 induction, A2 induction	Gibco^{TM}	300-01A-10UG
IL-1α	A1 induction	Gibco^{TM}	200-01A-2UG
IL-1β	A2 induction	Gibco^{TM}	200-01B-2UG
C1q	A1 induction	MilliporeSigma^{TM}	20-487-61MG
BMP4	Astrocyte differentiation	Gibco^{TM}	PHC9534
CNTF	Astrocyte differentiation	Gibco^{TM}	450-13-20UG
Dantrolene	TNFα release inhibition	Selleck Chemicals®	E4902
Salubrinal	TNFα release inhibition	Thermo Scientific^{TM} Chemicals	J64192.LB0
QIAGEN RNeasy Kit	RNA extraction	QIAGEN^{TM}	74104
High-Capacity RNA-to-cDNA Kit	cDNA synthesis	Applied Biosystems^{TM}	4387406
PowerTrack 2× SYBR Green Mix	RT-qPCR	Applied Biosystems^{TM}	A46109
Human TNFα ELISA Kit	TNFα quantification	Invitrogen^{TM}	KHC3013
Human iPSC-derived Neural Progenitor Cells (SCTi003-A)	Neural progenitor cells for experimentation and astrocyte differentiation	STEMCELL^{TM} Technologies	200-0620

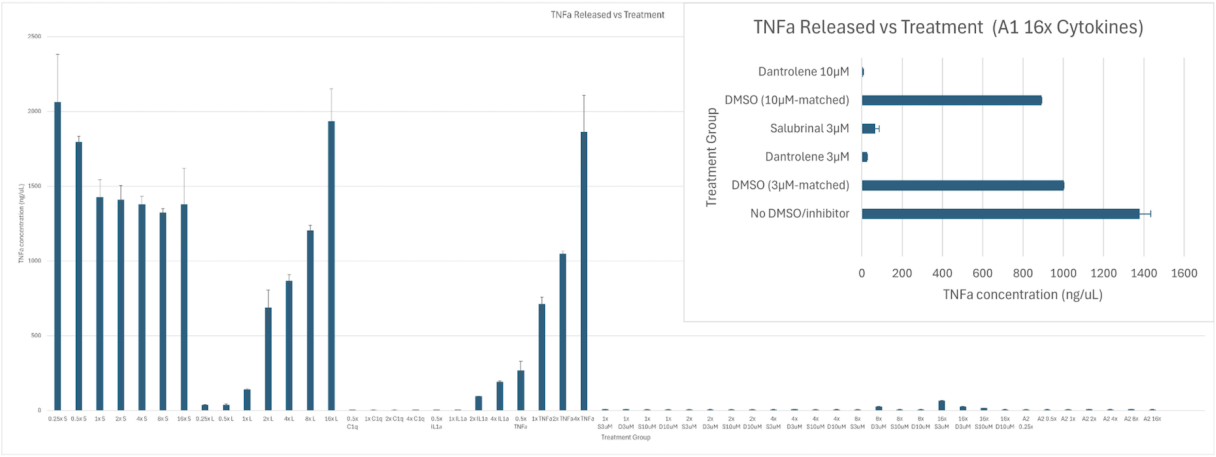

Figure. 7 TNFα release measured by ELISA across varying cytokine concentrations, combinations, and with inhibitors. "S" indicates the sample of media was collected 24 h after cytokines were removed, while "L" is indicative of 7 days. In the absence of either letter, the sample was taken at the 24 hour time point.

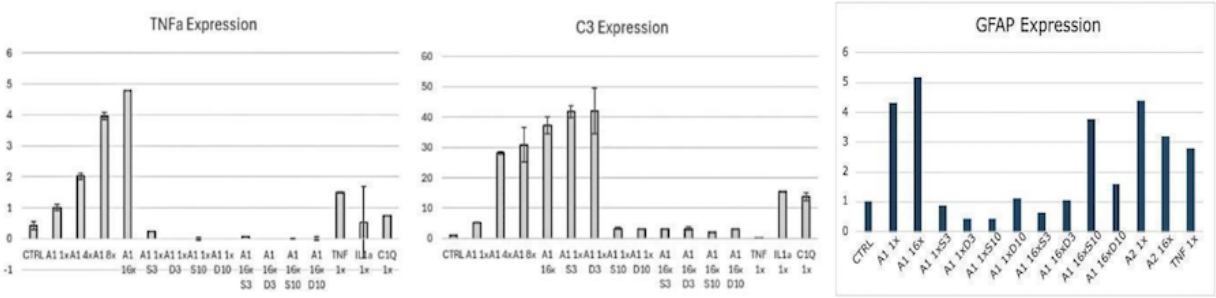

Figure. 8 RT-qPCR confirmed not only a reduction in TNFα expression but other inflammatory markers associated with A1 astrocytes after treatment with dantrolene or salubrinal.

OPC-associated markers, though lineage-tracing and functional myelination assays are needed to distinguish differentiation from transient state changes. Reactive astrocytes stimulated at higher concentrations of pro-inflammatory microglia-

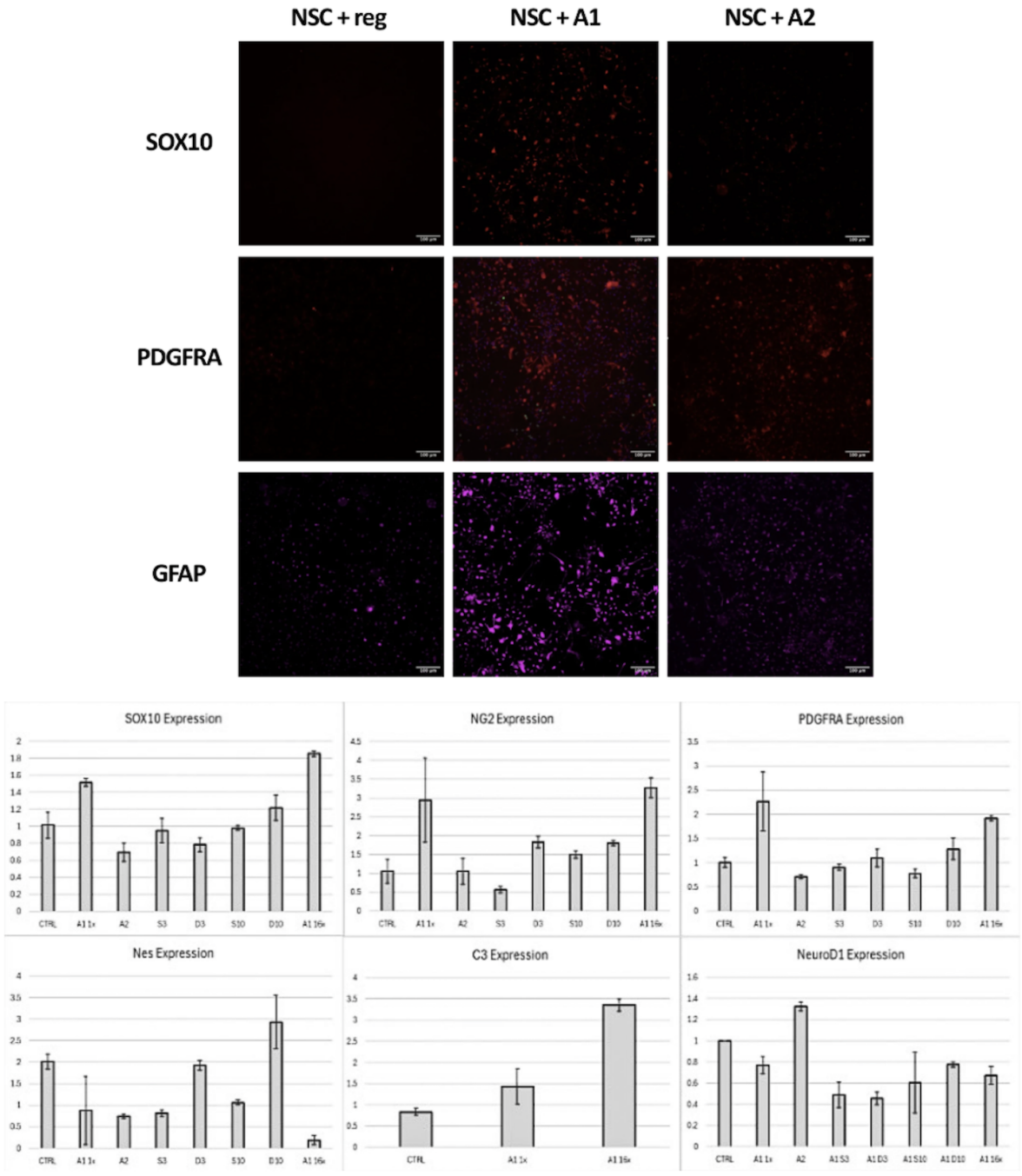

Figure. 9 Effect of astrocyte CM on NSC fate. (A) IF shows increased OPC marker expression (PDGFRA, SOX10) in NSCs treated with A1 astrocyte CM compared to homeostatic or A2 CM. (B) RT-qPCR supports upregulation of OPC-associated genes (SOX10, NG2, PDGFRA), which is reduced upon inhibitor treatment. Y-axis numbers represent fold change.

derived cytokines exhibited the most sustained TNFα release after one week, and TNFα alone was sufficient to induce robust TNFα production compared to IL-1α or C1q alone. A2 astrocytes generated with a combination of TNFα and IL-1β, showed no TNFα release, consistent with an antagonistic relationship between the two cytokines and supporting the in-

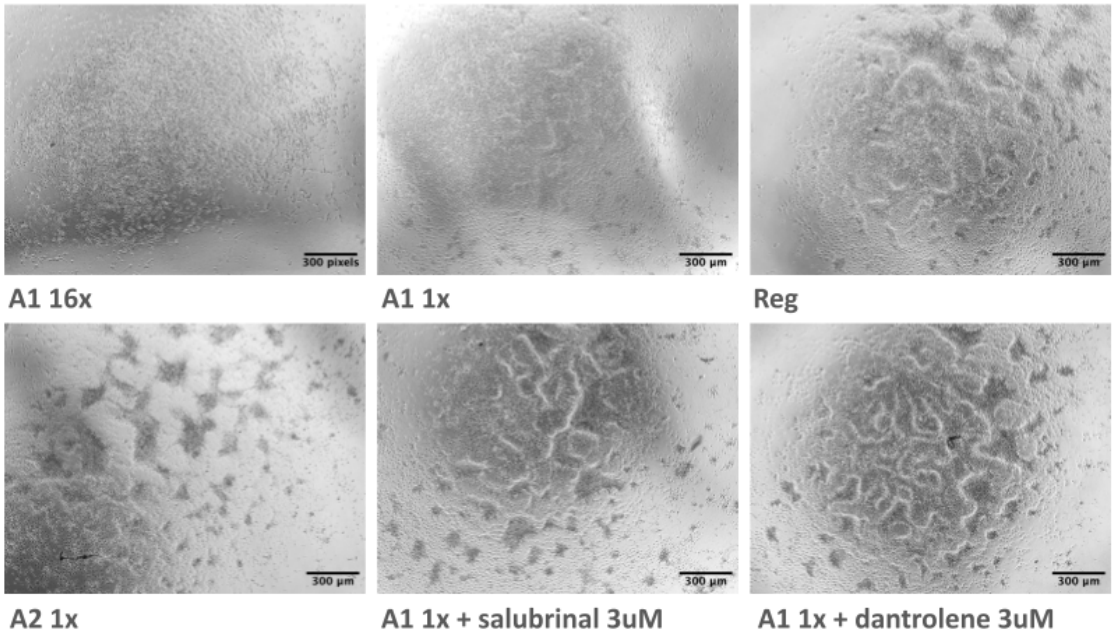

Figure. 10 NSCs given CM from homeostatic and A2 astrocytes as well as A1 astrocytes given salubrinal or dantrolene formed neurosphere-like aggregates on Matrigel, while not the A1-CM treated cells.

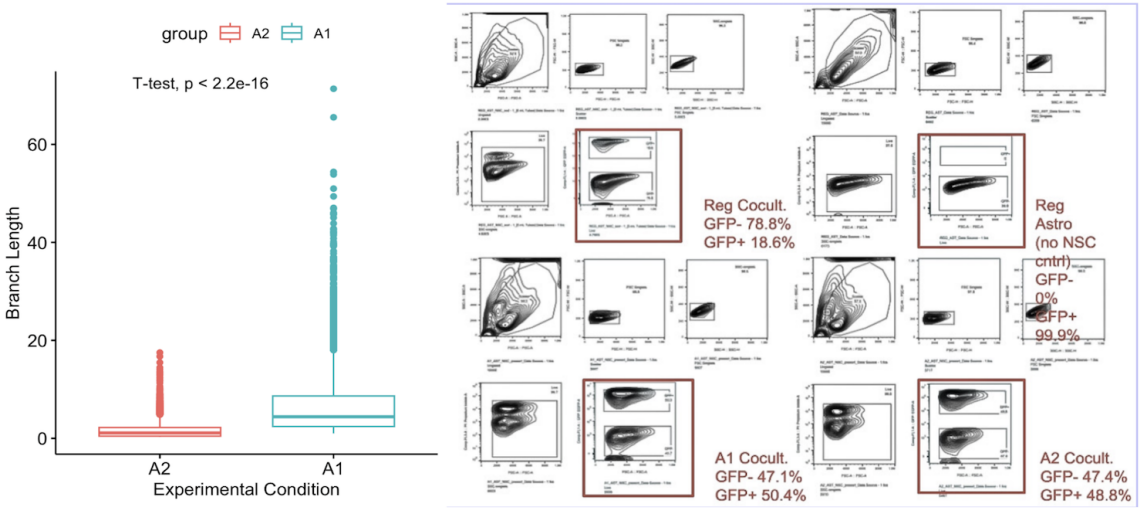

Figure. 11 (A) Average branch length of NSCs co-cultured with A2 and A1 astrocytes respectively. (B) A higher proportion of GFP^{+} cells was seen in A1 astrocyte co-cultures.

terpretation that the assay was not merely detecting residual exogenous TNFα. Acellular titration tests support that TNFα was effectively removed, but further experiments where neutralizing antibodies are added or an assay differentiating endogenous from recombinant ligand would further help confirm this claim. Administration of dantrolene and salubrinal for 24 h after the activation period successfully suppressed TNFα expression and release in reactive astrocytes, mitigating the effect seen on NSCs, which instead retained multipotent markers and neurosphere-forming qualities. To note is that accumulating evidence suggests the A1/A2 classification to be an oversimplification. Thus, "A1-like" and "A2-like" in the context of this study should be understood as heuristic rather than definite ends of a spectrum of reactive states,

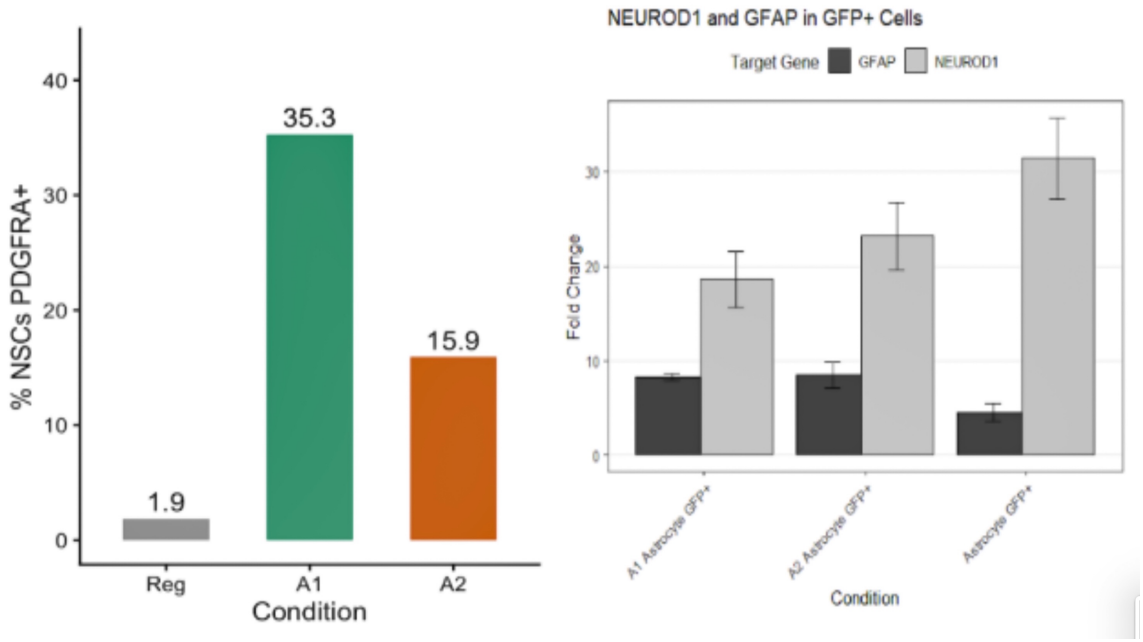

Figure. 12 (A) Percentage of NSCs expressing PDGFRA in cells co-cultured with homeostatic, A1, or A2 astrocytes. (B) NEURDO1 and GFAP expression in NSCs co-cultured with homeostatic, A1, or A2 astrocytes.

Table 5 Experimental workflow summary.

	Treatment	Control	Readout	Purpose
Exp 0: ScRNA-seq reanalysis	MCAO vs. sham mouse brains	Sham	Cell proportions, CellChat signaling	NSC/OPC abundance and signaling changes
Exp 1: NSCs + A1/A2 factors	A1 factors (TNFα + IL-1α + C1q); A2 factors (TNFα + IL-1β)	NSC media, blank differentiation media	IF (C3, GFAP, PDGFRA)	Effects of inflammatory cytokines on NSC fate
Exp 2: NSCs + individual factors	TNFα, IL-1α, C1q	NSC media	IF (PDGFRA, SOX10, C3, SOX2)	Effects of individual inflammatory cytokines on NSC fate
Exp 3: TNFα release by reactive astrocytes	Homeostatic, A1, A2 astrocytes; $\pm$ inhibitors	Homeostatic astrocytes; DMSO	ELISA, RT-qPCR	TNFα production and inhibitor effects
Exp 4: NSCs + astrocyte conditioned medium (CM)	CM from homeostatic, A1, A2 astrocytes; inhibitor-treated A1 CM	Homeostatic CM	IF, RT-qPCR	Effects of astrocyte-secreted factors on NSC differentiation
Exp 5: NSCs + reactive astrocyte co-cultures	A1, A2, homeostatic astrocytes	Homeostatic co-culture	Flow cytometry, morphology (branch length), IF, RT-qPCR	Contact-dependent effects on NSC differentiation

and reactive astrocyte responses likely demonstrate far more heterogeneity and context-dependence.

A limitation is that dantrolene and salubrinal could modulate other cytokines as well. A future experiment would be using an AAV vector with an Gfap-specific promoter to knock down TNFα in astrocytes, then comparing the effect of A1-activated astrocytes in which TNFα is knocked-down on NSC fate to regular A1 astrocytes. To better demonstrate the mechanism of A1 astrocytes recruiting NSCs to the site of the scar, a MCAO mouse model with AAV5-GfaAVC1D-TNFshRNA injected 2-3 weeks pre-injury could be combined with GFP$^+$ NSC transplantation and subsequent analysis of NSC recruitment to the lesion. Computational analysis relied on mouse scRNA data due to human ischemic stroke datasets containing insufficient numbers of NSCs to robustly analyze cell-cell communication. On the contrary, mouse datasets capture well-characterized NSC niches and provide multiple replicate time points to map NSC lineage progression and interactions. Cross-species differences in timing of NSC differentiation and inflammatory gene expression must be considered. Experiments are being repeated on primary cell lines. iPSC-derived cells show slightly differing inflammatory transcriptomic profiles as compared to primary cells[23]. Additionally, iPSC-derived astrocytes often retain a more fetal and immature state that lack robust expression of certain astrocyte markers such as AQP4 and ALDH1L1[24].

Additional cytotoxicity assays will quantify the effects of high cytokine doses and inhibitors beyond trypan blue counts. Co-cultures will be repeated at a lower seeding density (5k:5k) to avoid excessive astrocyte confluence. To better under-

stand the heterogeneity of reactive astrocytes[25] (with some uniquely presenting markers such as OLIG2 or Nestin) and how different methods of glial scar induction yield transcriptomically unique populations of reactive astrocytes, organoid models will be used. Brain organoids typically see the appearance of glial cells between days 60-90, and at this time point organoids will be either injected with LPS, administered supernatant from A1 astrocytes, or kept in hypoxic conditions mimicking ischemia. Then, Flow Cytometry and single-cell sequencing may be applied to identify unique subtypes of reactive astrocytes. From there further experiments will measure their TNFα producing capacity and effect on NSCs.

Vanishing White Matter Disease (VWMD) is a condition in which astrocytes fail to activate and take on the typical A1 inflammatory subtype due to mutations in genes encoding subunits of eukaryotic translation initiation factor 2B (eIF2B)[26]. A lack of glial scarring is seen in VWMD, with oligodendrocytes and OPCs failing to home to the site of the glial scar despite the presence of major lesions to the white matter[27]. Analyzing a bulk RNA-seq dataset from an eIF2B knockout, the same drastic reduction in the NSC population that is seen in wild type populations that have undergone an event provoking glial scar formation is not demonstrated. This suggests that by impairing astrocytes in their ability to activate, their effects on NSC differentiation is inhibited, reducing a population that would normally contribute to proper formation of the architecture of the glial scar.

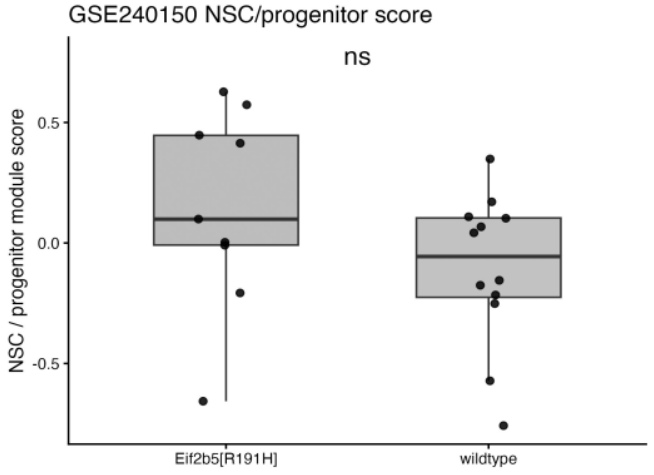

Figure. 13 In a mouse model of the disease, neural stem cell (NSC) proportions remain unchanged after injury (Welch's t-test, p = 0.154 $>$ 0.05).

While there are instances of excessive glial scarring and reactive astrogliosis leading to deleterious effects on axon regeneration and neuronal toxicity, the signaling axis between A1 reactive astrocytes and NSCs to form C3[3] OPCs may be instrumental in forming the protective barrier that the glial scar provides. Thus, clinical emphasis should be placed on modulating rather than inhibiting the activation of A1 astrocytes, and seeking to better understand how we may exploit their protective functions in containing damage and facilitating remyelination.

References

1 I. B. Wanner and M. A. Anderson and B. Song and J. Levine and A. Fernandez and Z. Gray-Thompson and Y. Ao and M. V. Sofroniew, Glial Scar Borders Are Formed by Newly Proliferated, Elongated Astrocytes That Interact to Corral Inflammatory and Fibrotic Cells via STAT3-Dependent Mechanisms After Spinal Cord Injury. Journal of Neuroscience. Vol. 33, No. 31, pp. 12870–12886, 2013., https://doi.org/10.1523/JNEUROSCI.2121-13.2013.

2 A. Buss and K. Pech and B. A. Kakulas and D. Martin and J. Schoenen and J. Noth and G. A. Brook, NG2 and Phosphacan Are Present in the Astroglial Scar After Human Traumatic Spinal Cord Injury. BMC Neurology. Vol. 9, No. 1, 2009., https://doi.org/10.1186/1471-2377-9-32.

3 J. Kjell and M. Götz, Filling the Gaps – A Call for Comprehensive Analysis of Extracellular Matrix of the Glial Scar in Region- and Injury-Specific Contexts. Frontiers in Cellular Neuroscience. Vol. 14, 2020., https://doi.org/10.3389/fncel.2020.00032.

4 R. Hu and J. Zhou and C. Luo and J. Lin and X. Wang and X. Li and X. Bian and Y. Li and Q. Wan and Y. Yu and H. Feng, Glial Scar and Neuroregeneration: Histological, Functional, and Magnetic Resonance Imaging Analysis in Chronic Spinal Cord Injury. Journal of Neurosurgery: Spine. Vol. 13, No. 2, pp. 169–180, 2010., https://doi.org/10.3171/2010.3.SPINE09190.

5 L. Cheng et al., M1-Type Microglia Can Induce Astrocytes to Deposit Chondroitin Sulfate Proteoglycan After Spinal Cord Injury. Neural Regeneration Research. Vol. 17, No. 5, p. 1072, 2022., https://doi.org/10.4103/1673-5374.324858.

6 L. Henning and H. Antony and A. Breuer and J. Müller and G. Seifert and E. Audinat and P. Singh and F. Brosseron and M. T. Heneka and C. Steinhäuser and P. Bedner, Reactive Microglia Are the Major Source of Tumor Necrosis Factor Alpha and Contribute to Astrocyte Dysfunction and Acute Seizures in Experimental Temporal Lobe Epilepsy. Glia. Vol. 71, No. 2, pp. 168–186, 2022., https://doi.org/10.1002/glia.24265.

7 M. Bhatt and M. Sharma and B. Das, The Role of Inflammatory Cascade and Reactive Astrogliosis in Glial Scar Formation Post-Spinal Cord Injury. Cellular and Molecular Neurobiology. Vol. 44, No. 1, p. 78, 2024., https://doi.org/10.1007/s10571-024-01519-9.

8 Y.-Y. Fan and J. Huo, A1/A2 Astrocytes in Central Nervous System Injuries and Diseases: Angels or Devils? Neurochemistry International. Vol. 148, p. 105080, 2021., https://doi.org/10.1016/j.neuint.2021.105080.

9 Y. Su and Z. Chen and H. Du and R. Liu and W. Wang and H. Li and B. Ning, Silencing miR-21 Induces Polarization of Astrocytes to the A2 Phenotype and Improves the Formation of Synapses by Targeting Glypican 6 via the STAT3 Pathway After Acute Ischemic Spinal Cord Injury. The FASEB Journal. Vol. 33, No. 10, pp. 10859–10871, 2019., https://doi.org/10.1096/fj.201900743r.

10 S. A. Liddelow and K. A. Guttenplan and L. E. Clarke and F. C. Bennett and C. J. Bohlen and L. Schirmer and M. L. Bennett and A. E. Münch and W.-S. Chung and T. C. Peterson and D. K. Wilton and A. Frouin and B. A. Napier and N. Panicker and M. Kumar and M. S. Buckwalter and D. H. Rowitch and V. L. Dawson and T. M. Dawson and B. Stevens, Neurotoxic Reactive Astrocytes Are Induced by Activated Microglia. Nature. Vol.

541, No. 7638, pp. 481–487, 2017., https://doi.org/10.1038/nature21029.

11 L. M. Delgado-García and A. C. Ojalvo-Sanz and E. Nakamura and E. Martín-López and M. Porcionatto and L. Lopez-Mascaraque, Dissecting Reactive Astrocyte Responses: Lineage Tracing and Morphology-Based Clustering. Biological Research. Vol. 57, No. 1, 2024., https://doi.org/10.1186/s40659-024-00532-y.

12 M. Y. Batiuk and A. Martirosyan and J. Wahis and F. de Vin and C. Marneffe and C. Kusserow and J. Koeppen and J. F. Viana and J. F. Oliveira and T. Voet and C. P. Ponting and T. G. Belgard and M. G. Holt, Identification of Region-Specific Astrocyte Subtypes at Single Cell Resolution. Nature Communications. Vol. 11, No. 1, 2020., https://doi.org/10.1038/s41467-019-14198-8.

13 D. Ye et al., Identifying Genes That Affect Differentiation of Human Neural Stem Cells and Myelination of Mature Oligodendrocytes. Cellular and Molecular Neurobiology. Vol. 43, No. 5, pp. 2337–2358, 2022., https://doi.org/10.1007/s10571-022-01313-5.

14 O. Gonzalez-Perez, Neural Stem Cells in the Adult Human Brain. Biological and Biomedical Reports. Vol. 2, No. 1, pp. 59–69, 2012., https://pmc.ncbi.nlm.nih.gov/articles/PMC3505091.

15 K. Ioannidis et al., 3D Reconstitution of the Neural Stem Cell Niche: Connecting the Dots. Frontiers in Bioengineering and Biotechnology. Vol. 9, p. 705470, 2021., https://doi.org/10.3389/fbioe.2021.705470.

16 A. L. Soung and V. A. Davé and C. Garber and E. D. Tycksen and L. L. Vollmer and R. S. Klein, IL-1 Reprogramming of Adult Neural Stem Cells Limits Neurocognitive Recovery After Viral Encephalitis by Maintaining a Proinflammatory State. Brain, Behavior, and Immunity. Vol. 99, pp. 383–396, 2022., https://doi.org/10.1016/j.bbi.2021.10.010.

17 J. Wang et al., Inhibition of A1 Astrocytes and Activation of A2 Astrocytes for the Treatment of Spinal Cord Injury. Neurochemical Research. Vol. 48, No. 3, pp. 767–780, 2023., https://doi.org/10.1007/s11064-022-03820-9.

18 H. Li et al., Targeting Astrocytes Polarization After Spinal Cord Injury: A Promising Direction. Frontiers in Cellular Neuroscience. Vol. 18, 2024., https://doi.org/10.3389/fncel.2024.1478741.

19 F. Li and T. Hayashi and G. Jin and K. Deguchi and I. Nagotani and I. Nagano and M. Shoji and P. H. Chan and K. Abe, The Protective Effect of Dantrolene on Ischemic Neuronal Cell Death Is Associated with Reduced Expression of Endoplasmic Reticulum Stress Markers. Brain Research. Vol. 1048, No. 1–2, pp. 59–68, 2005., https://doi.org/10.1016/j.brainres.2005.04.058.

20 A. Ovcjak and A. Xiao and J.-S. Kim and B. Xu and V. Szeto and E. Turlova and A. Abussaud and N. Chen and S. P. Miller and H.-S. Sun and Z.-P. Feng, Ryanodine Receptor Inhibitor Dantrolene Reduces Hypoxic-Ischemic Brain Injury in Neonatal Mice. Experimental Neurology. Vol. 351, p. 113985, 2022., https://doi.org/10.1016/j.expneurol.2022.113985.

21 X. Fan and J. Chen and Z. Zhang and F. Chen and H. Wang and Y. Cai and J. Li, Salubrinal Alleviates Traumatic Spinal Cord Injury Through Suppression of the eIF2α/ATF4 Pathway in Mouse Model. BIOCELL. Vol. 46, No. 6, pp. 1527–1535, 2022., https://doi.org/10.32604/biocell.2022.018269.

22 J. V. Welser-Alves and R. Milner, Microglia Are the Major Source of TNF-α and TGF-β1 in Postnatal Glial Cultures; Regulation by Cytokines, Lipopolysaccharide, and Vitronectin. Neurochemistry International. Vol. 63, No. 1, pp. 47–53, 2013., https://doi.org/10.1016/j.neuint.2013.04.007.

23 A.-S. Spreng and M. Brüll and H. Leisner and I. Suciu and M. Leist, Distinct and Dynamic Transcriptome Adaptations of iPSC-Generated Astrocytes After Cytokine Stimulation. Cells. Vol. 11, No. 17, p. 2644, 2022., https://doi.org/10.3390/cells11172644.

24 B. Szeky and V. Jurakova and E. Fouskova and A. Feher and M. Zana and V. R. Karl and J. Farkas and M. Bodi-Jakus and M. Zapletalova and S. Pandey and R. Kucera and J. Lochman and A. Dinnyes, Efficient Derivation of Functional Astrocytes from Human Induced Pluripotent Stem Cells (hiPSCs). PLOS ONE. Vol. 19, No. 12, e0313514, 2024., https://doi.org/10.1371/journal.pone.0313514.

25 M. A. Anderson and Y. Ao and M. V. Sofroniew, Heterogeneity of Reactive Astrocytes. Neuroscience Letters. Vol. 565, pp. 23–29, 2014., https://doi.org/10.1016/j.neulet.2013.12.030.

26 S. Dooves and M. Bugiani and N. L. Postma and E. Polder and N. Land and S. T. Horan and A.-L. F. van Deijk and A. van de Kreeke and G. Jacobs and C. Vuong and J. Klooster and M. Kamermans and J. Wortel and M. Loos and L. E. Wisse and G. C. Scheper and T. E. M. Abbink and V. M. Heine and M. S. van der Knaap, Astrocytes Are Central in the Pathomechanisms of Vanishing White Matter. Journal of Clinical Investigation. Vol. 126, No. 4, pp. 1512–1524, 2016., https://doi.org/10.1172/JCI83908.

27 M. Geva and Y. Cabilly and Y. Assaf and N. Mindroul and L. Marom and R. Gali and D. Pinchasi and O. Elroy-Stein, A Mouse Model for Eukaryotic Translation Initiation Factor 2B Leucodystrophy Reveals Abnormal Development of Brain White Matter. Brain. Vol. 133, No. 8, pp. 2448–2461, 2010., https://doi.org/10.1093/brain/awq180.